Environmental Science and Ecotechnology 19 (2024) 100334

Contents lists available at ScienceDirect

Environmental Science and Ecotechnology

journal homepage: www.journals.elsevier.com/environmental-science-and-ecotechnology/

Original Research

Salinity causes differences in stratigraphic methane sources and sinks

Ying Qu [a], Yuxiang Zhao [a], Xiangwu Yao [a], Jiaqi Wang [a], Zishu Liu [a], Yi Hong [b], Ping Zheng [a], Lizhong Wang [b, **], Baolan Hu [a, c, *]

[a] Department of Environmental Engineering, Zhejiang University, Hangzhou, China
[b] Ocean College, Zhejiang University, Zhoushan, China
[c] Zhejiang Province Key Laboratory for Water Pollution Control and Environmental Safety, Hangzhou, China

ARTICLE INFO

Article history:
Received 24 March 2023
Received in revised form
9 October 2023
Accepted 12 October 2023

Keywords:
Shallow gas strata
Salinity
Methane emission
Microbial community
Microbial interactions

ABSTRACT

Methane metabolism, driven by methanogenic and methanotrophic microorganisms, plays a pivotal role in the carbon cycle. As seawater intrusion and soil salinization rise due to global environmental shifts, understanding how salinity affects methane emissions, especially in deep strata, becomes imperative. Yet, insights into stratigraphic methane release under varying salinity conditions remain sparse. Here we investigate the effects of salinity on methane metabolism across terrestrial and coastal strata (15–40 m depth) through *in situ* and microcosm simulation studies. Coastal strata, exhibiting a salinity level five times greater than terrestrial strata, manifested a 12.05% decrease in total methane production, but a staggering 687.34% surge in methane oxidation, culminating in 146.31% diminished methane emissions. Salinity emerged as a significant factor shaping the methane-metabolizing microbial community's dynamics, impacting the methanogenic archaeal, methanotrophic archaeal, and methanotrophic bacterial communities by 16.53%, 27.25%, and 22.94%, respectively. Furthermore, microbial interactions influenced strata system methane metabolism. Metabolic pathway analyses suggested Atribacteria JS1's potential role in organic matter decomposition, facilitating methane production via Methanofastidiosales. This study thus offers a comprehensive lens to comprehend stratigraphic methane emission dynamics and the overarching factors modulating them.

1. Introduction

Methane, the second most abundant global greenhouse gas, has 28 times the global warming potential of carbon dioxide (CO_2) [1]. Methane concentrations in the atmosphere have been on the rise since 2007, with global averages exceeding 1900 ppb, representing approximately threefold the pre-industrial level [2,3]. These emissions stem from various sources, with geological being the fourth largest source, accounting for 37.5 Mt yr^{-1} [4]. Organic-rich shallow gas strata are widely distributed in terrestrial plains and coastal areas [5–8], and often leak methane due to environmental disturbances. Therefore, from the perspective of preventing engineering risks and mitigating the greenhouse effect, methane emissions from shallow gas strata cannot be neglected.

The natural methane cycle is driven by microorganisms. Methanogenic and methanotrophic archaea belonging to the phylum Euryarchaeota and methanotrophic bacteria belonging to the phyla Proteobacteria and Verrucomicrobia are the main participants [9–11]. Methanogenic and methanotrophic archaea include eight orders: Methanococcales, Methanopyrales, Methanobacteriales, Methanosarcinale, Methanomicrobiales, Methnocellales, Methanomassiliicoccales, and '*Candidatus* Methanophagales' [12]. Previous studies have shown that methanogens can use H_2/CO_2, acetate, methanol/methylamines, and methoxylated aromatic compounds as substrates to produce CH_4 [13,14]. Recent findings indicate that they can also directly oxidize long-chain alkanes and participate in methane metabolism through the beta-oxidation and Wood–Ljungdahl pathways [15]. Anaerobic methane-oxidizing archaea (ANME) oxidize methane through reverse methanogenesis. ANME consists of three groups: ANME-1 (subclusters a and b), ANME-2 (subclusters a/b, c, and d), and ANME-3 [16]. ANME can utilize electron acceptors, such as NO_3^-, NO_2^-, SO_4^{2-}, Mn^{4+}, Fe^{3+}, As^{5+}, and humic substances, to oxidize methane [17–19]. In

* Corresponding author. Department of Environmental Engineering, Zhejiang University, Hangzhou, China.
** Corresponding author.
E-mail addresses: wanglz@zju.edu.cn (L. Wang), blhu@zju.edu.cn (B. Hu).

https://doi.org/10.1016/j.ese.2023.100334

addition, ANME communities have been reported to exist in ecosystems such as terrestrial mud volcanoes and deep marine sediments [17–21]. In recent years, researchers have also found methanogenic potential in several non-Euryarchaeotal lineages, including Bathyarchaeia, Methanomethylicia, Nitrososphaeria, Heimdallarchaeia, and Korarchaeia [22–26].

Clarifying the mechanisms of microbial community assembly is essential for studying community ecology. Microbial community assembly is determined by a combination of deterministic and stochastic processes [27]. Deterministic processes are related to ecological selection mechanisms, including biotic factors (interspecies interactions) and abiotic factors (environmental filtering) [28]. On the other hand, stochastic processes reflect the randomness of changes in the relative abundance of species, including random birth, death, dispersal, and drift processes [29]. Co-occurrence networks have been extensively applied to study the potential microbial interactions that affect community composition and ecosystem function, providing supporting information on microbial ecology [30,31]. A dense microbial co-occurrence network offers an easy and efficient series of interactions for metabolism, signal exchange, and electron transfer between microorganisms [32]. Based on the co-occurrence network analysis of methanogens from 39 paddy soils, researchers found that commonly co-occurring methanogenic groups interacted more closely and contributed more to methane emissions [33]. In the molecular network constructed from black-odorous water sediment communities, positive interactions between fermenters, syntrophs, and methanogens indicated the possible promotion of continuous conversion of organic matter to methane [34]. Another network analysis study emphasized the strong link between methanogenesis and anaerobic oxidation of methane (AOM) pathways, which is crucial for balancing the methane cycle [35].

Environmental factors also play a key role in methane metabolism. It has been found that an increase in pH reduced the ability of forest and rangeland soils to absorb methane, thereby inducing the transition from methane sink to methane source [36]. Organic matter content, moisture, electron acceptor type, and concentration affect methane metabolism [9,37]. Salinity also significantly impacts ecosystem CO_2 and methane fluxes [38]. As salinity increased, methane emissions were shown to decrease in tidal marshes [39], coastal wetlands [40], and brackish freshwater wetlands [41]. Consequently, salinity has generally been used as a predictor of methane emissions [42]. Salinity affects the microbial processes of methane emissions mainly through sulfate reduction effects and ionic effects [41,43]. In tidal wetlands, the sulfate in seawater often inhibits methanogenesis due to the thermodynamically favorable nature of sulfate reduction processes over methanogenesis [42]. In addition, salinity has been reported to regulate methane emissions by affecting the structure and abundance of methanogenic archaeal communities [44]. In recent years, saltwater intrusion has increased salinity in coastal habitats through surface or subsurface flows, increasing selection pressure on microbial communities and affecting biogeochemical cycles [45]. Although studies on methane metabolism in different saline habitats have been conducted, they have only focused on shallow sediments (<1 m depth) [9,44,46], and little has been done regarding methane metabolism and the associated microbial mechanisms in strata. Overall, microbially driven methane metabolism in strata of different salinities deserves our attention.

This study investigates the effect of salinity on stratigraphic methane metabolism and provides a new perspective on its profiling by applying *in situ* studies, microcosm simulation experiments, and omics analysis.

2. Materials and methods

2.1. Study sites and sample collection

In August 2020, two 40-m deep stratigraphic soil columns were collected from terrestrial (30°18′ N, 120°22′ E) and coastal (30°31′ N, 121°99′ E) sites, respectively (Fig. S1). The terrestrial strata site was located in the southern part of Hangzhou Bay. Hangzhou Bay is a typical estuarine bay that receives plentiful terrestrial substrates, and its shore area was formed by siltation after a series of sea invasions and retreats. The coastal strata site was located in the Zhoushan Islands. The Zhoushan Islands are on the southern edge of the modern Yangtze River submerged delta and are an important channel for the interchange of sediment between Hangzhou Bay and the East China Sea. The strata comprised marine sandy gravel layers and silt beach accumulation, with a distinct stratigraphic marine nature [47]. The high deposition rates and abundant substrates create rich, shallow gas reservoir environments in both areas, providing a typical case study of methane metabolism. As the top 0–15 m of the strata was artificially filled with rocks, we selected soil column samples from 15 to 40 m depth as the study object. A total of 100 samples were gathered, with ten samples obtained at 5-m intervals. Each sample was divided into two parts: one portion was stored at 4 °C for physicochemical and activity experiments, while the other at −80 °C for molecular biology experiments.

2.2. Physicochemical measurement

The pH values were determined by a pH meter (FE20, Mettler-Toledo, Switzerland) after extracting the strata samples with water (5:1 water-soil ratio). Iron and manganese content was determined by inductively coupled plasma mass spectrometry (ICP–MS) [48]. Moisture was measured by the gravimetric method as described previously [49]. The soil organic matter (OM) content was determined by the potassium dichromate oxidation method with air-dried soils. NO_2^-, NO_3^-, and SO_4^{2-} were extracted by water (5:1 water-soil ratio), and their concentrations were measured by ion chromatography (Dionex ICS-1000, USA). NH_4^+ was extracted using 2 mol L^{-1} KCl (5:1 solution-soil ratio) and determined by spectrophotometry (APHA, 2017). Traditionally, soil salinity is commonly measured by the electrical conductivity (ECe) of the saturated soil leachate [50]. Therefore, the strata salinity was determined by a salinity meter (FieldScout ECC 450 Meter, USA) after extracting the strata samples with water (5:1 water-soil ratio).

2.3. Methane production, oxidation, and emission potential measurement

In this study, 25 g of strata samples were measured into 250 mL serum bottles. Deionized water was subsequently added to the liquid level at 100 mL, reserving 150 mL of head space. These sample bottles were then flushed with argon for 10 min before being placed in a shaking incubator (150 rpm) at a constant temperature of 20 °C and kept in the dark. After one day of pre-incubation, methane in the headspace was measured by gas chromatograph-mass spectrometry (Agilent 7890A inert MSD 5977B, Agilent, USA) every 12 h [51]. The potential methane production and oxidation rates were calculated by the linear regression of gas over time (Text S1). The potential methane emission rate at each depth was determined by the methane production rate minus the methane oxidation rate.

2.4. DNA extraction, sequence processing, and quantitative PCR (qPCR)

DNA was extracted from samples of the two strata using the DNeasy Powersoil Kit (QIAGEN, Germany) following the manufacturer's instructions [52]. The V4–V5 region of bacterial 16S rRNA genes was amplified using the 515-F (5′-GTGCCAGCMGCCGCGG-3′) and 907-R (5′-CCGTCAATTCMTTTRAGTTT-3′) primer pair [53]. The V4–V5 region of archaeal 16S rRNA genes was amplified using the 515-F (5′-CAGCCGCCGCGGTAA-3′) and 915-R (5′-GTGCTCCCCCGCCAATTCCT-3′) primer pair [54]. PCR was conducted in a total volume of 25 μL with 12.5 μL 2 × SYBR GREEN (Takara, Japan), 1 μL forward primer (20 mM), 1 μL reverse primer (20 mM), 1 μL template DNA and 9.5 μL RNase-free Water (Takara, Japan). PCR conditions for bacterial 16S rRNA gene amplification were as follows: 94 °C for 2 min; 30 cycles of 94 °C for 30 s, 60 °C for 30 s, and 72 °C for 45 s; and a final extension at 72 °C for 5 min. While PCR conditions for archaeal 16S rRNA gene amplification were as follows: 95 °C for 5 min; 40 cycles of 95 °C for 30 s, 57 °C for 30 s, and 72 °C for 30 s; and a final extension at 72 °C for 8 min. Then, the amplicons were visualized on 2% agarose gels and purified using the SanPrep Column PCR Product Purification Kit (Sangon Biotech, Shanghai, China). Purified amplicons were subsequently sent for Ion Torrent sequencing at Zhejiang University. Raw sequence data were processed using QIIME 2 software (v2021.4). DADA2 was used to filter and trim sequences, correct errors, and remove chimeras [55]. With a similarity threshold based on 100%, clean reads were clustered into amplicon sequence variants (ASV), each of which was annotated to a specific taxon by comparison with the Genome Taxonomy Database (GTDB) (v2.3.2) using BLAST. The qPCR analyses were performed on iCycler iQ5 (Bio-Rad, USA). Details of the primers can be found in Table S1.

2.5. Metagenomic assembly, binning, and annotation

Metagenome sequencing was performed on the Illumina HiSeq2500 platform. For metagenomic assembly of strata samples, the raw data was de-duplicated and trimmed using Trimmomactic (v0.39) [56]. The *de novo* splicing and assembly of the clean data was subsequently completed using MEGAHIT (v1.0), and contigs with splice lengths greater than 250 bp in the samples were selected for binning to obtain the metagenome-assembled genomes (MAGs) [57]. Bins with completeness greater than 50% and contamination less than 10% were selected as good bins by CheckM (v1.0.7) [58], and the species were classified according to the GTDB (v2.3.2). Sequences from all good bins were subjected to rRNA gene prediction using Barrnap (v0.9). Unigenes (non-redundant gene catalog) were obtained after running Linclust [59]. The Unigene sequences were compared with the GTDB (v2.3.2) database for species annotation and combined with gene abundance to obtain species composition and abundance information. The predicted gene protein sequences were compared with the KEGG database to obtain functional annotation information, followed by functional gene frequency determination using DIAMOND (v0.8.35) with an *e*-value of 10^{-5} [60].

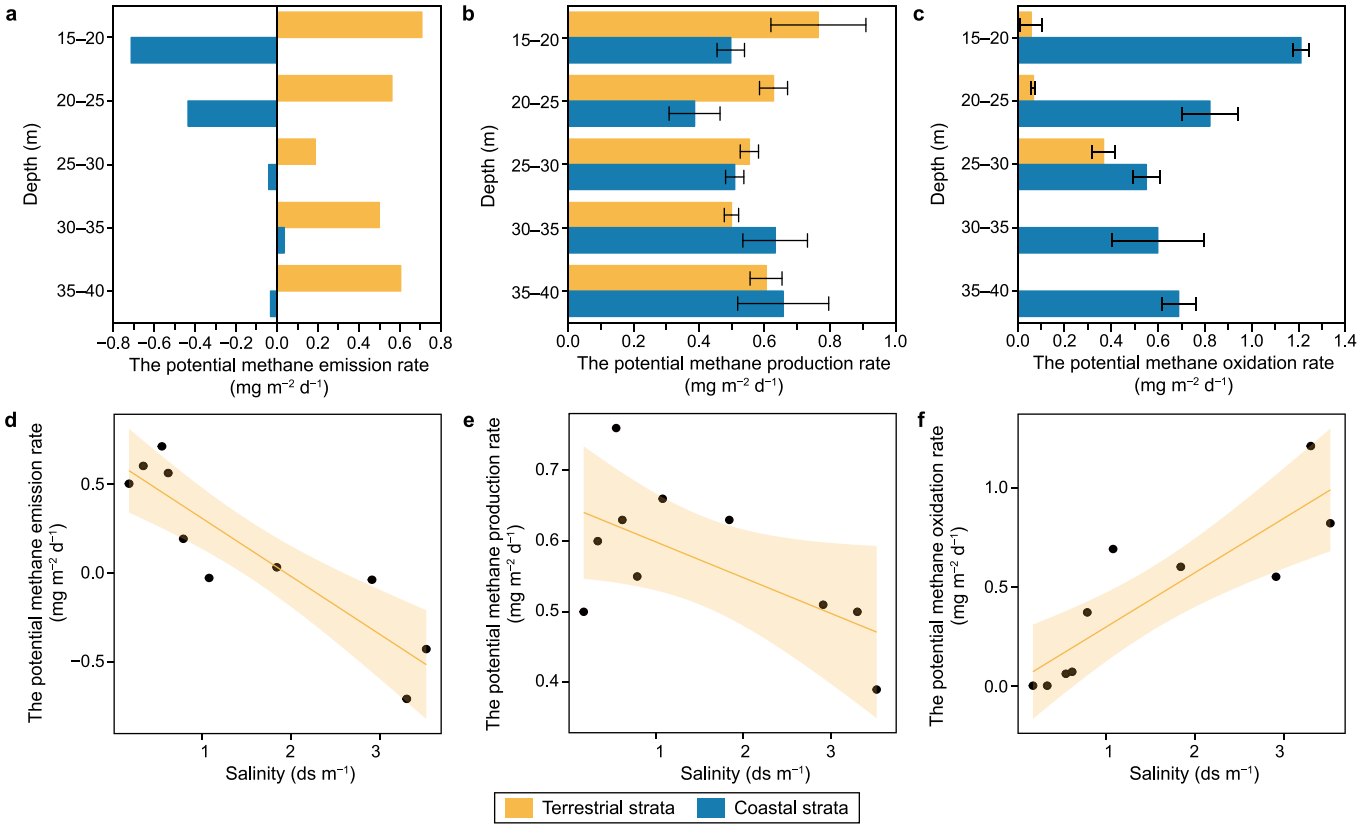

Fig. 1. The effect of salinity on methane metabolism in terrestrial strata and coastal strata. **a**–**c**, The potential methane emission rate (**a**), methane production rate (**b**), and methane oxidation rate (**c**). **d**–**f**, Fitting curves of salinity and the potential methane emission rate (**d**), methane production rate (**e**), and methane oxidation rate (**f**), including a 95 % confidence interval.

2.6. Statistical analysis

To determine the mechanism of microbial community assembly, the contribution of each ecological process was quantified using the iCAMP R package [61]. To explore the abiotic factors driving the differences in methane-metabolizing archaeal communities between the two strata and to further determine the contribution and significance of these abiotic factors to community variation, Redundancy Analysis (RDA) was performed using the *vegan* and *rdacca.hp* R packages [62], while Variance Partitioning Analysis (VPA) was performed using the *vegan* R packages. Co-occurrence networks were constructed to explore microbial interactions in the strata based on Spearman correlation using the *ggClusterNet* R package [30,63]. Spearman correlation coefficient >0.8 and *p*-value <0.001 were set to select data. One hundred random networks created by randomly rewiring all nodes and links were also calculated to verify the reliability of constructed networks [64–66]. Gephi (v0.9.2) was applied to achieve the visualization of co-occurrence networks. Differences in physicochemical parameters, methane flux, and microbial relative abundance in the two strata were assessed using a one-way analysis of variance (ANOVA). Potential relationships between salinity and methane flux, ecological processes, and gene abundance were analyzed by Pearson correlation analysis. All data analyses were performed in IBM SPSS 23 (SPSS Inc., USA).

3. Results

3.1. Physicochemical parameters of strata

The physicochemical parameters of the two strata are shown in Table S2. As the depth increased, the pH of both strata showed a decreasing trend, while moisture did not change significantly. There was no significant difference in iron and manganese content between the two strata, but the trends were different. With increasing depth, iron and manganese content showed a decreasing trend in the terrestrial strata, while a gradual increasing trend was observed in the coastal strata. The NH_4^+ content of terrestrial and coastal strata ranged from 1.40 to 142.08 mg kg^{-1} and 17.80–37.19 mg kg^{-1}, respectively. The NO_2^- content ranged from 3.94 to 17.24 mg kg^{-1} and 5.67–28.34 mg kg^{-1}, respectively. The NH_4^+ and NO_2^- content were both at low levels compared to the other measured parameters. OM, salinity, NO_3^-, and SO_4^{2-} of the terrestrial and coastal strata showed significant differences ($p < 0.05$). The mean OM, salinity, NO_3^-, and SO_4^{2-} contents of the coastal strata were 9.60 g kg^{-1}, 2.52 ds m^{-1}, 562.10 mg kg^{-1}, and 412.73 mg kg^{-1}, respectively, representing 1.96, 5.11, 13.42, and 14.12 times higher than those of the terrestrial strata (4.90 g kg^{-1}, 0.49 ds m^{-1}, 41.87 mg kg^{-1}, and 29.22 mg kg^{-1}).

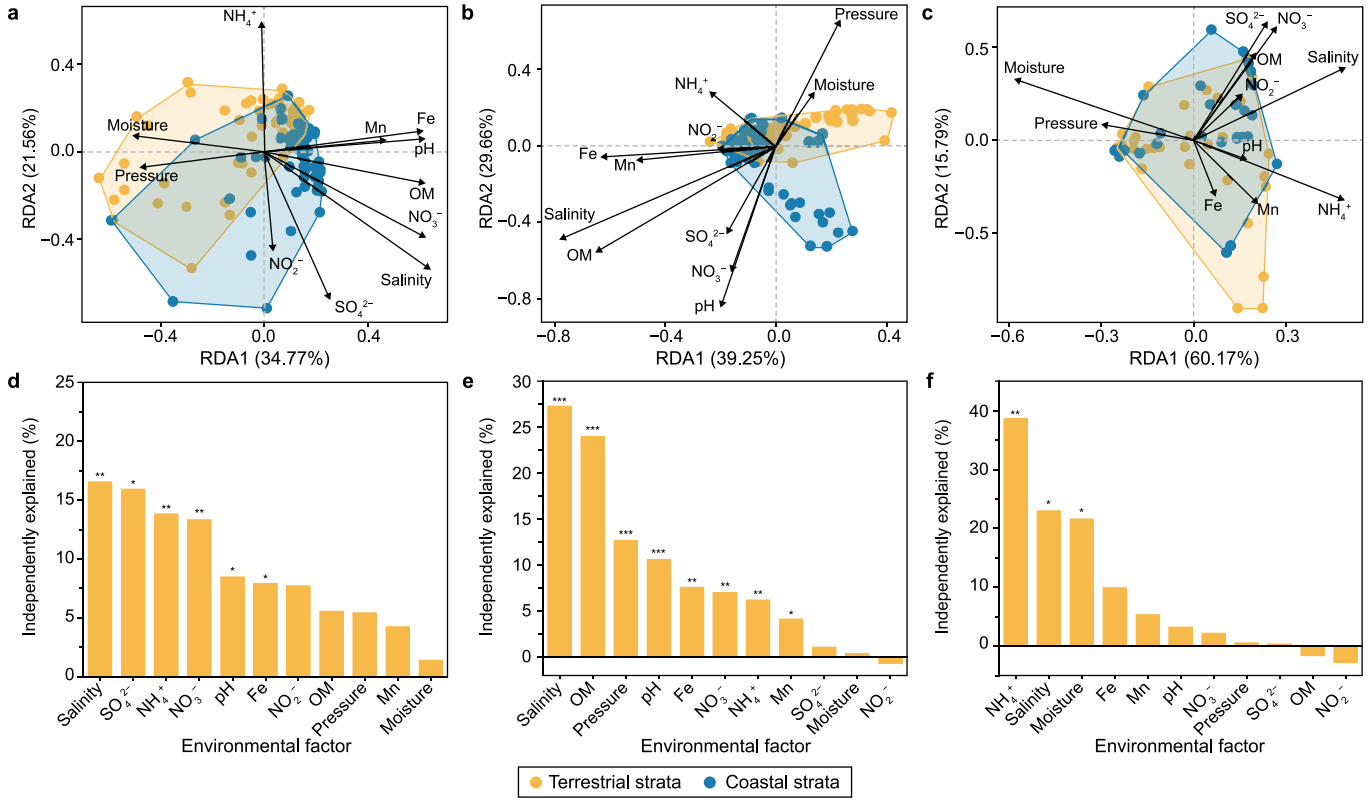

Fig. 2. Redundancy analysis (RDA) of environmental factors of methane metabolizing microbial communities in terrestrial and coastal strata. **a**–**c**, RDA of environmental factors of methanogenic communities (**a**), methane-oxidizing archaeal communities (**b**), and methane-oxidizing bacterial communities (**c**). **d**–**f**, Independent explanation of environmental factors to methanogenic communities (**d**), methane-oxidizing archaeal communities (**e**), and methane-oxidizing bacterial communities (**f**). *, **, and *** indicate significant differences at the 0.05, 0.01, and 0.001 levels, respectively.

3.2. Methane production, oxidation, and emission rates

The potential methane emission rates from the two strata showed significant differences ($p < 0.01$) (Fig. 1a). The total potential methane emission rate from the terrestrial strata was 2.56 mg m^{-2} d^{-1}, indicating a potential methane source. The total potential methane emission rate from the coastal strata was −1.18 mg m^{-2} d^{-1}, indicating a potential methane sink. The difference in potential methane production rates between the two strata was not significant (Fig. 1b). The total potential methane production rate from the terrestrial strata was 3.05 mg m^{-2} d^{-1}, while the total potential methane production rate from the coastal strata was 2.68 mg m^{-2} d^{-1}. However, the difference in potential methane oxidation rates was significant ($p < 0.01$) (Fig. 1c). The total potential methane oxidation rate from the terrestrial strata was 0.49 mg m^{-2} d^{-1}, while the total potential methane oxidation rate from the coastal strata was 3.87 mg m^{-2} d^{-1}. Compared to terrestrial strata, coastal strata had a 12.05% lower total methane production rate, but a 687.34% higher total methane oxidation rate, resulting in a 146.31% lower total methane emission. Pearson correlation analysis showed that salinity was negatively correlated with the potential methane production rate and significantly negatively correlated with the potential methane emission rate ($p < 0.001$), while it was significantly positively correlated with the potential methane oxidation rate ($p < 0.01$) (Fig. 1d–f), indicating the importance of salinity on methane emissions.

3.3. Methane metabolizing microbial community structure

To analyze the dynamics of microbial communities in terrestrial and coastal strata, the relative importance of different ecological factors in microbial assembly was quantified by iCAMP. The results indicated that deterministic processes dominated microbial community assembly in terrestrial and coastal strata (Fig. S2a and b). In the terrestrial strata, homogeneous selection (55.97%) dominated archaeal community assembly, and dispersal limitation (43.36%) dominated bacterial community assembly (Fig. S2c and e). In the coastal strata, homogeneous selection was the main influence on community assembly for archaea (76.51%) and bacteria (43.65%) (Fig. S2d and f). Salinity was the dominant abiotic factor in archaeal community assembly. With increasing salinity, archaeal homogeneous selection gradually strengthened ($p < 0.01$), while bacterial dispersal limitation gradually weakened ($p < 0.05$) (Fig. S2g and h). To further explore the effect of salinity on the stratigraphic methane-metabolizing microorganisms, RDA analysis was applied (Fig. 2). It revealed that salinity was a strong driver of differences in the methanogenic archaeal community and methanotrophic archaeal community between terrestrial and coastal strata, contributing 16.53% ($p < 0.01$) of variation in the methanogenic archaeal community and 27.25% ($p < 0.001$) of variation in the methanotrophic archaeal community between the two strata. For methanotrophic bacterial community variation, NH_4^+ had the largest contribution at 38.65% ($p < 0.01$), followed by salinity at 22.94% ($p < 0.05$). In the strata, methanotrophic archaea (contribution rate, 42%) contributed 8.4 times more to AOM than methanotrophic bacteria (contribution rate, 5%), dominating the methane oxidation process (Fig. S3). A total of four methanogenic groups and four ANME subgroups were detected in the strata: Methanobacteriales, Methanomassiliicoccales, Methanosarciniales, and Methanofastidiosales, and ANME-1a, ANME-1b, ANME-2a/b, and ANME-2d, respectively (Fig. S4). According to qPCR results (Fig. 3), the average 16S rRNA copy number of methanogens in terrestrial strata was 2.22 × 10^6 copies g^{-1}, 1.28 times higher than in coastal strata (1.74 × 10^6 copies g^{-1}) ($p > 0.05$). The average 16S rRNA copy number of ANMEs in coastal strata was 5.99 × 10^6 copies g^{-1}, 4.51 times higher than in terrestrial strata (1.33 × 10^6 copies g^{-1}) ($p > 0.05$), indicating that AOM was more active in the coastal strata. Pearson correlation analysis showed that the abundance of ANME-1 ($p < 0.01$), ANME-2d ($p < 0.01$), and ANMEs ($p < 0.01$) increased significantly with increasing salinity (Table S3), suggesting that salinity would affect the abundance of ANMEs.

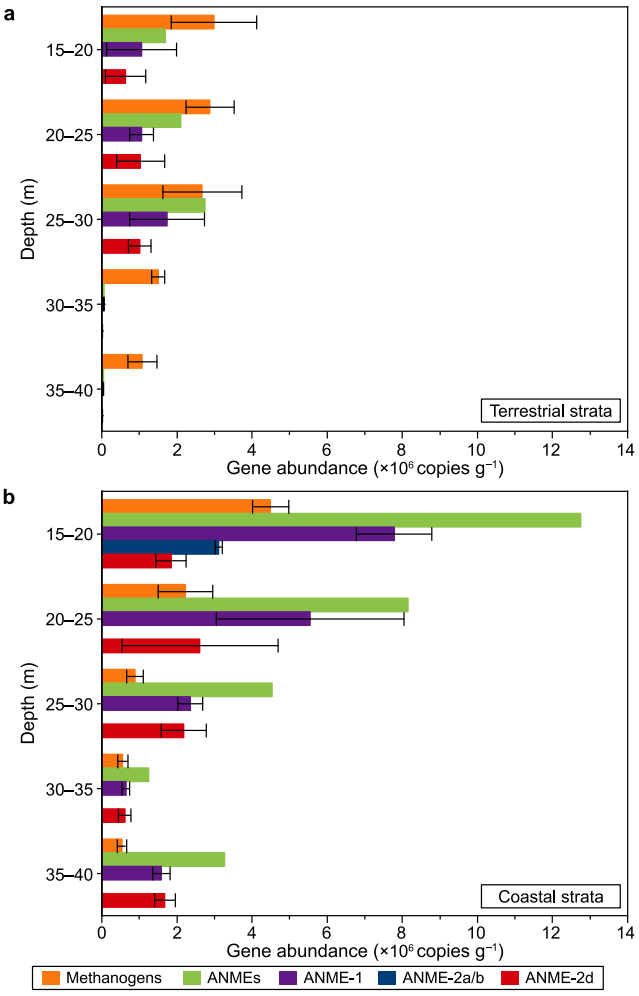

Fig. 3. 16S rRNA gene abundance of methanogens, ANME-1, ANME-2a/b, ANME-2d, and ANMEs in the strata. **a**, Terrestrial strata. **b**, Coastal strata.

3.4. Methane metabolism functional gene distribution

The distribution of functional genes for methane metabolism in terrestrial and coastal strata is shown in Fig. 4. Annotation of KEGG gene functions indicated that the *pmo* and *fdo* functional genes were absent from the aerobic methane oxidation pathway in both strata, suggesting that the strata mainly underwent AOM. With increasing depth in terrestrial strata, *mcr* gene abundance increased to a maximum at 20–25 m, then decreased to a minimum at 30–35 m, and then increased again at 35–40 m. In contrast, *mer*, *mtd*, *mch*, *ftr*, and *fwd* gene abundances showed a decreasing trend, then increasing, and then decreasing again, while *mtr* gene abundance increased to a maximum at 25–30 m and then gradually decreased. In coastal strata, *mcr* gene abundance first decreased with increasing depth, then increased to a maximum at 25–30 m and decreased to a minimum at 35–40 m. In contrast, *mtr*, *mch*, and *fwd* gene abundances increased initially, followed by a decrease, but then increased again. The trends in *mer* and *mtd* gene

abundances were similar, higher at 20–25 and 30–35 m, while *ftr* gene abundance showed a slowly increasing trend with depth. The abundance of *ftr* genes was highest at all depth intervals in both strata, while the abundance of *mcr* genes was lowest at all depth intervals. The total abundance of methane metabolism functional genes was 1.42 times higher in the coastal strata (3.84×10^{-3}) than in the terrestrial strata (2.71×10^{-3}). Among the methane metabolism functional genes, the abundances of *mtr*, *mer*, *mtd*, *mch*, *ftr*, and *fwd* genes in the coastal strata were 1.68×10^{-4}, 6.63×10^{-4}, 5.07×10^{-4}, 7.27×10^{-4}, 1.17×10^{-4}, and 5.98×10^{-4}, respectively, which were 1.43 ($p < 0.05$), 1.50 ($p < 0.01$), 1.81 ($p < 0.001$), 1.31 ($p > 0.05$), 1.39 ($p < 0.05$), and 1.29 ($p > 0.05$) times higher those in the terrestrial strata. In contrast, the abundance of *mcr* functional genes encoding the key enzyme for methane metabolism was only 0.6 times ($p > 0.05$) higher than in the terrestrial strata. Pearson correlation analysis demonstrated that salinity was significantly positively correlated with *mtr* ($p < 0.001$), *mer* ($p < 0.01$), and *mtd* ($p < 0.001$) gene abundance, suggesting that salinity may influence methane metabolism by regulating methane metabolism gene abundance (Table S4).

3.5. Microbial interactions

Based on 16S rRNA gene sequences from the 100 samples, we constructed respective co-occurrence networks of archaea from the terrestrial and coastal strata to reveal potential interactions between methane-metabolizing archaea and other archaea (Fig. S5a and b). In the terrestrial co-occurrence network, methanogens were not linked to other archaea, whereas ANME showed potential interactions with Thermoproteota, Hadarchaeota, and Asgardarchaeota. In the coastal co-occurrence network, neither methanogens nor ANME interacted with other archaea. Topological characteristics of the co-occurrence networks displayed a 21.11% reduction in network size (total number of nodes), a 51.28% reduction in number of edges, a 38.34% reduction in average degree and a 6.1% increase in modularity in the coastal strata compared to the terrestrial strata, indicating that increased salinity attenuated the complexity of the co-occurrence network in the coastal strata and weakened the interactions between archaea (Fig. S5c–f).

Using metagenomic analysis, 19 terrestrial and 22 coastal archaeal MAGs were reconstructed. Further annotation of the MAGs with KEGG revealed five terrestrial archaeal MAGs and four coastal archaeal MAGs were associated with methane metabolism. Among these, a MAG belonging to the Methanofastidiosales was only detected in the terrestrial strata and possessed some genes from the hydrogenotrophic and acetoclastic methanogenic pathways (Fig. 5a). Among the 35 and 32 bacterial MAGs reconstructed from terrestrial and coastal strata, respectively, JS1 bacteria, belonging to the phylum Atribacteria were found to likely interact with methanogens (Fig. 5c,f). JS1 MAGs contained various monosaccharide, polysaccharide, and amino acid ABC transporter protein genes, as well as enzymes involved in glycolysis and fermentation, indicating that JS1 bacteria had the potential to produce acetate and CO_2 from the fermentation of organic matter. Additionally, genes encoding membrane-bound hydrogenases (Mbh), which can produce H_2 using electrons provided by reduced ferroredoxin to reduce H^+, were identified in the JS1 MAGs. H_2, CO_2, and acetate are small molecules that can act as interspecies electron shuttles to Methanofastidiosales to produce methane as substrates. Methane is oxidized by reverse methanogenesis in the presence of several enzymes (Mcr, Mtr, Mer, Mtd, Mch, Ftr, and Fwd). The MAG of ANME-1-THS was found in both terrestrial and coastal strata. Genes in the AOM pathway and genes encoding electron bifurcation complexes were more complete in the MAG of the ANME-1-THS from coastal strata than that of the terrestrial strata (Fig. 5b,e). The MAG belonging to Methanosarcinales, which was only detected in coastal samples, possessed a complete AOM pathway and was classified as ANME-2a/b based on energy metabolism mechanisms and phylogenetic comparisons (Fig. 5d). In addition to traditional methanogens, we also found that Methanomethylicia, Nitrososphaeria, and Lokiarchaeia may be involved in the methane metabolic process through different pathways (Fig. S6).

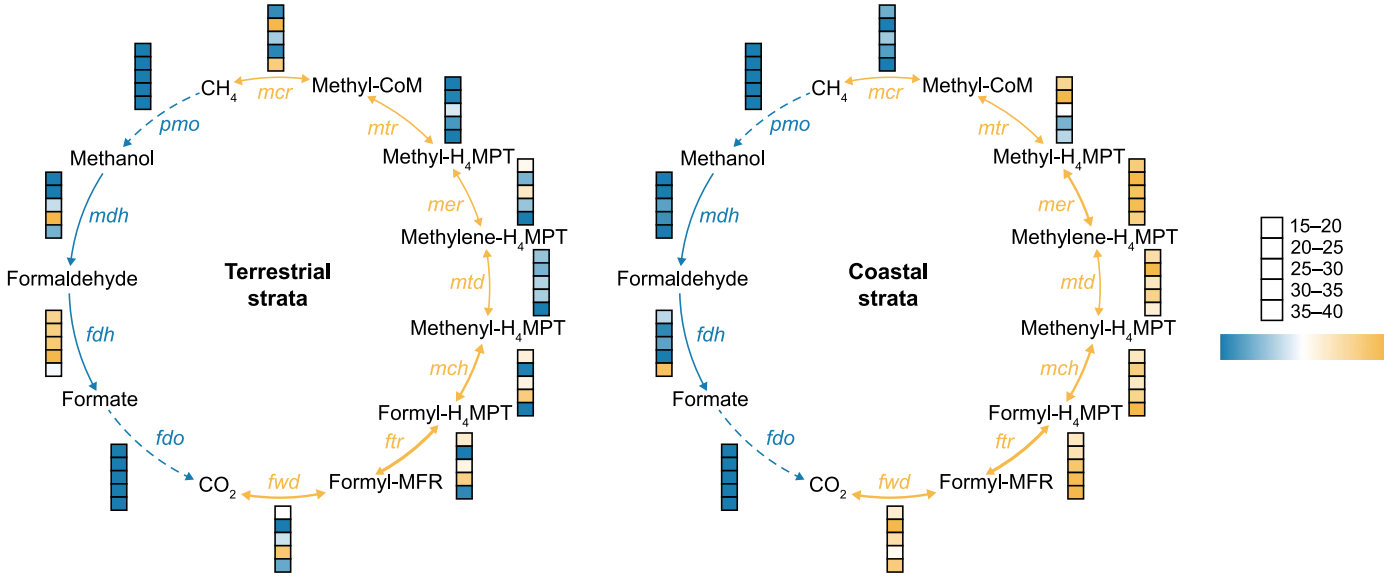

Fig. 4. The abundance of genes involved in methane metabolism of samples collected from terrestrial and coastal strata. The yellow lines represent both methanogenesis and AOM, while the blue lines represent the aerobic methane oxidation process. The color of an individual block reflects the abundance of a gene at a certain depth, with blue and yellow indicating significantly lower and higher abundance, respectively. The thickness of the line represents the size of the sum of the gene abundance. *mcr*, methyl coenzyme-M reductase gene; *mtr*, tetrahydromethanopterin S-methyltransferase gene; *mer*, F_{420}-dependent methylenetetrahydromethanopterin dehydrogenase gene; *mtd*, methylene– tetrahydromethanopterin reductase gene; *mch*, methenyltetrahydromethanopterin cyclohydrolase gene; *ftr*, formylmethanofuran-tetrahydromethanopterin N-formyltransferase gene; *fwd*, formylmethanofuran dehydrogenase gene; *fdo*, formate dehydrogenase iron-sulfur subunit gene; *fdh*, formate dehydrogenase gene; *mdh*, malate dehydrogenase gene; *pmo*, methane/ammonia monooxygenase.

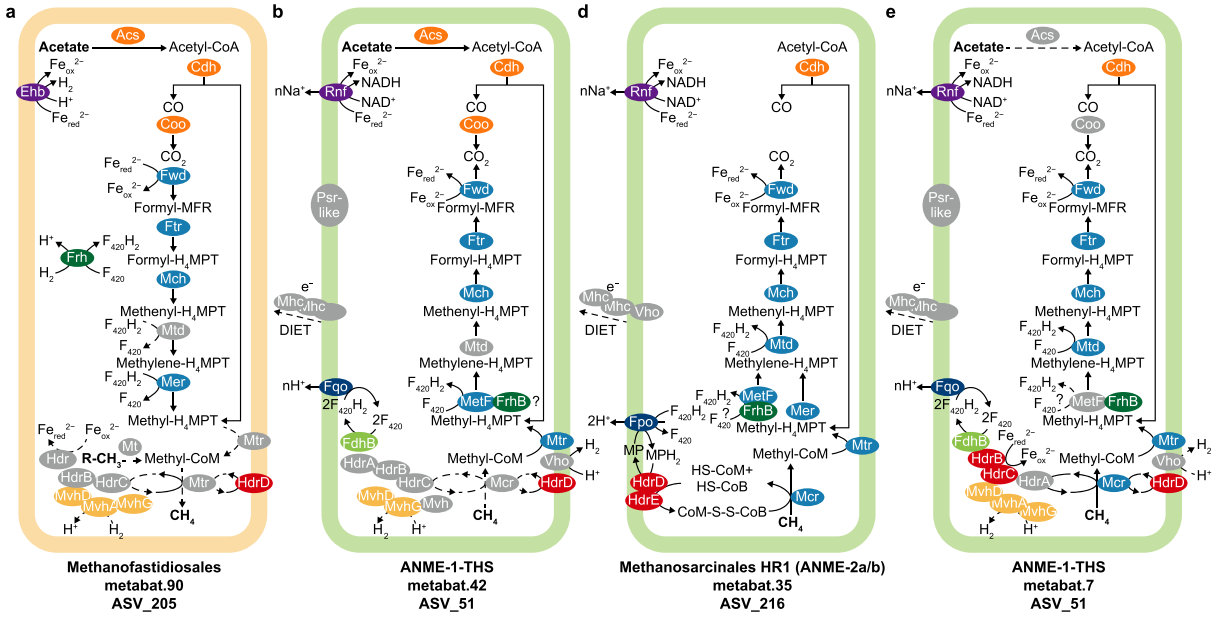
a
b
d
e
Acetate
Acetyl-CoA
Acs
Cdh
CO
Coo
Fwd
Formyl-MFR
Ftr
Formyl-H4MPT
Mch
Methenyl-H4MPT
Mtd
Methylene-H4MPT
Mer
Methyl-H4MPT
Mtr
Methyl-CoM
Mcr
Ehb
Frh
Mtl
Hdr
R-CH3
HdrB
HdrC
MvhB
MvhA
MvhC
Mtc
HdrD
CH4
Rnf
NADH
NAD+
nNa+
Psr-like
e-
MhcAhc
DIET
Fqo
FdhB
HdrA
MetF
FrhB
Vho
Fpo
MP
MPH2
HdrE
HS-CoM+
HS-CoB
CoM-S-S-CoB
Methanofastidiosales
metabat.90
ASV_205
ANME-1-THS
metabat.42
ASV_51
Methanosarcinales HR1 (ANME-2a/b)
metabat.35
ASV_216
ANME-1-THS
metabat.7
ASV_51

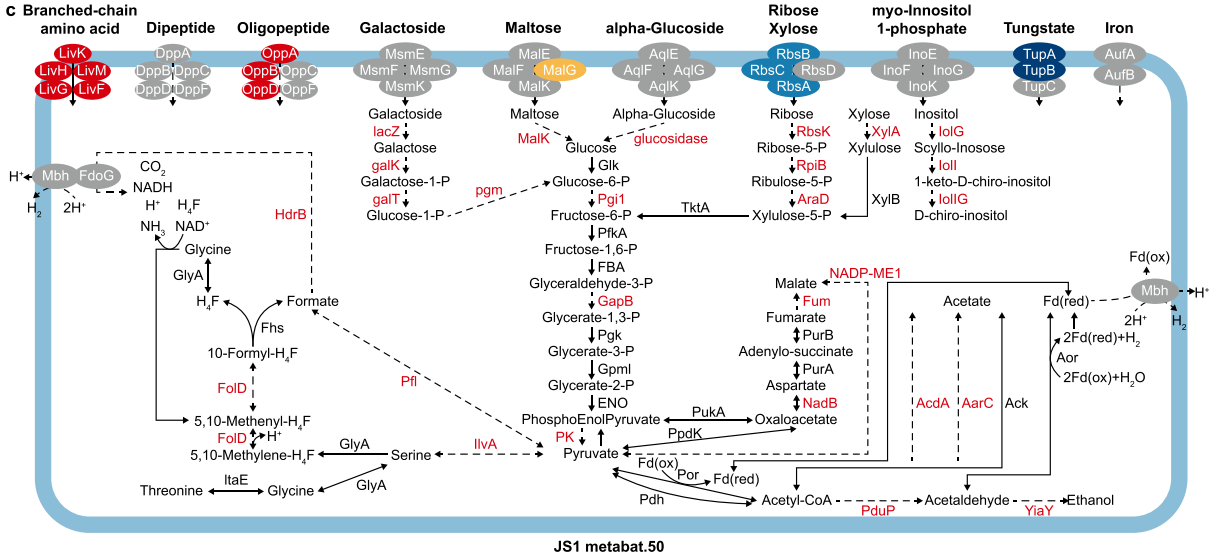
c Branched-chain amino acid
Dipeptide
Oligopeptide
Galactoside
Maltose
alpha-Glucoside
Ribose Xylose
myo-Innositol 1-phosphate
Tungstate
Iron
LivK
LivH
LivM
LivG
LivF
DppA
DppB
DppC
DppD
DppF
OppA
OppB
OppC
OppD
OppF
MsmE
MsmF
MsmG
MsmK
MalE
MalF
MalG
MalK
AglE
AglF
AglG
AglK
RbsB
RbsC
RbsD
RbsA
InoE
InoF
InoG
InoK
TupA
TupB
TupC
AufA
AufB
Galactoside
lacZ
Galactose
galK
Galactose-1-P
galT
Glucose-1-P
Maltose
Alpha-Glucoside
glucosidase
Glucose
Ribose
RbsK
Ribose-5-P
RpiB
Ribulose-5-P
AraD
Xylulose-5-P
Xylose
XylA
Xylulose
XylB
Inositol
IolG
Scyllo-Inosose
IolI
1-keto-D-chiro-inositol
IolIG
D-chiro-inositol
pgm
Glucose-6-P
Pgi1
Fructose-6-P
TktA
PfkA
Fructose-1,6-P
FBA
Glyceraldehyde-3-P
GapB
Glycerate-1,3-P
Pgk
Glycerate-3-P
Gpml
Glycerate-2-P
ENO
PhosphoEnolPyruvate
PK
Pyruvate
PukA
Oxaloacetate
PpdK
Mbh
FdoG
CO2
NADH
H+
H4F
NH3
NAD+
HdrB
Glycine
GlyA
Formate
Fhs
10-Formyl-H4F
FolD
5,10-Methenyl-H4F
5,10-Methylene-H4F
GlyA
Serine
IlvA
Threonine
ItaE
Glycine
GlyA
Pfl
Malate
NADP-ME1
Fum
Fumarate
PurB
Adenylo-succinate
PurA
Aspartate
NadB
Oxaloacetate
Fd(ox)
Fd(red)
Mbh
2H+
H2
2Fd(red)+H2
Aor
2Fd(ox)+H2O
Acetate
AcdA
AarC
Ack
Pdh
Por
Acetyl-CoA
PduP
Acetaldehyde
YiaY
Ethanol
JS1 metabat.50
ASV_1082

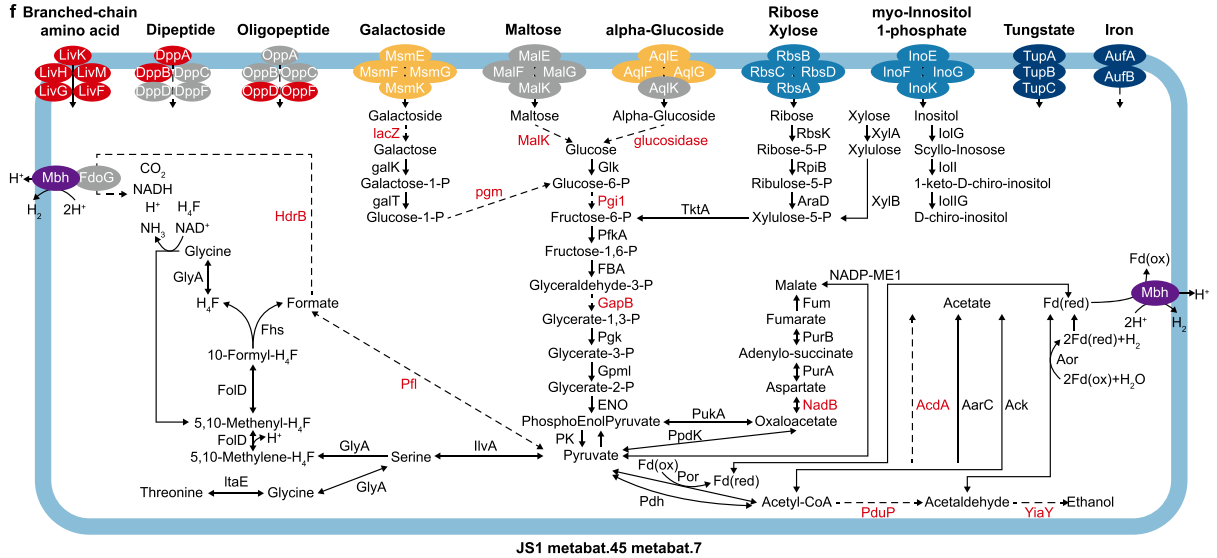
f Branched-chain amino acid
Dipeptide
Oligopeptide
Galactoside
Maltose
alpha-Glucoside
Ribose Xylose
myo-Innositol 1-phosphate
Tungstate
Iron
JS1 metabat.45 metabat.7
ASV_1082

Methanomethylicia may produce methane via the methylotrophic pathway, and Nitrososphaeria may produce methane via the hydrogenotrophic and methylotrophic pathways. Lokiarchaeia from the coastal strata may produce methane via the hydrogenotrophic and methylotrophic pathways. Lokiarchaeia from the terrestrial strata possessed the *mcr* gene for methane metabolism and a methane oxidation pathway similar to that of ANME-1-THS. However, because it had a partial genetic deletion, we cannot be sure whether it is undergoing methanogenesis or methane oxidation.

The 16S rRNA sequences of the above MAGs were aligned with the high-throughput 16S rRNA data to obtain species with >97% similarity and to compare their relative abundance in terrestrial and coastal strata (Fig. S7). According to the results, Methanofastidiosales and *Candidatus* Caldiarchaeum were possibly important drivers of methanogenesis in the terrestrial strata. The total relative abundance of Methanofastidiosales in the terrestrial strata was 1.05×10^{-3}, 90 times higher than that of the coastal strata (1.17×10^{-5}) ($p > 0.05$). The total relative abundance of *Candidatus* Caldiarchaeum in the terrestrial strata was 8.73×10^{-2}, 1.48 times higher than that of the coastal strata (5.89×10^{-2}) ($p < 0.05$). In contrast, the total relative abundance of ANME−2a/b in the terrestrial strata (3.51×10^{-5}) was only 0.08 times that of the coastal strata (4.56×10^{-4}) ($p > 0.05$).

4. Discussion

4.1. Effect of salinity on methane emission

The current study found that the terrestrial shallow gas strata were a source of methane, while the coastal shallow gas strata were a sink of methane. The total methane emission from terrestrial strata was 2.56 mg m^{-2} d^{-1} (Fig. 1a), lower than that from paddy soils (6.24 mg m^{-2} d^{-1}) and Zoige peatlands (50.40 mg m^{-2} d^{-1}) [67], but higher than that from forest soils (0.30 mg $m^{-2}d^{-1}$) [68], while total methane emission from coastal strata was similar to those from mangroves [69,70]. Rising salinity was the most obvious difference between the terrestrial and coastal strata, and it determined the large differences in methane emissions (Fig. 1a,d). Methanogenesis has been negatively correlated with salinity in various habitats, which was consistent with our findings (Fig. 1e). This may be because high salinity reduces methanogenic activity and decreases methane production [71]. However, the total methane production rate was only 12.05% lower in coastal strata, with five times higher salinity levels than in terrestrial strata (Fig. 1a and Table S2). One possible reason is that while methanogenesis is inhibited by SO_4^{2-} reduction at higher SO_4^{2-} concentrations, this effect is attenuated by high levels of organic matter [72]. In addition, the concentration of the electron acceptors NO_3^- and SO_4^{2-} increased with increasing salinity, promoting AOM [73], thus resulting in a 687.34% higher total methane oxidation rate and 146.31% lower total methane emission in the coastal strata as compared with the terrestrial strata (Fig. 1a,c).

4.2. Effect of salinity on methane metabolizing microorganisms

In this study, salinity was the key abiotic factor affecting methane emissions from the strata. It is not only a dominant player in archaeal community assembly (Fig. S2) but also an important driver of differences in the methane-metabolizing microbial communities of both strata (Fig. 2). Salinity is crucial for microbial community assembly [74], and it can influence the diversity, composition, and co-occurrence networks of archaeal and bacterial communities along with pH, shaping the mechanisms of community assembly [75]. The results demonstrated a significant positive correlation between salinity and the relative contribution of homogeneous selection in the stratigraphic archaeal community assembly (Fig. S2g), suggesting that salinity drove the stratigraphic archaeal community assembly in a deterministic manner. Due to the diffusive effect of seawater flow [76], the coastal strata were subject to stronger salinity filtering than terrestrial strata, leading to a higher degree of impact by deterministic processes on archaeal communities.

In general, higher salinity would limit water use by microorganisms and produce high osmotic stress [77]. However, archaea in coastal habitats are generally adapted to marine environments, and a certain degree of salinity stress may promote archaeal community activity [75,78]. ANME-1 and ANME-2a/b are widely distributed in marine environments and often participate in sulfate-dependent AOM together with bacteria. Meanwhile, ANME-2d is mainly distributed in freshwater habitats and involved in various AOMs, such as nitrate-dependent AOM and metal-dependent AOM [21]. The higher availability of NO_3^- and SO_4^{2-} shaped the coastal strata ANME community, resulting in higher abundances of ANME-1 and ANME-2d exercising sulfate-dependent AOM and nitrate-dependent AOM (Fig. 3), which is in line with previous studies [21]. Researchers observed that part of the genome of ANME-1 in Lost Hammer Spring contained homologous osmotic stress response genes. This would indicate that ANME-1 is more likely to survive in high-salt environments than the other subgroups [79]. The same situation may have also contributed to the higher average abundance of ANME-1 in coastal strata compared to terrestrial strata (Fig. 3). Through metagenomic analysis, this study reconstructed the terrestrial lineage ANME-1-THS (Fig. 5b,e). Lacking the multihaeme c-type cytochromes (MHCs), ANME-1-THS cannot undergo direct interspecific electron transfer and may grow without syntrophs [80]. When the relative concentrations of reactants and products change, the direction of chemical reactions in the methanogenesis and AOM reverse accordingly [81,82]. ANME-1 has been described as being engaged in methanogenesis in marine sediments in a previous study [82]. Similarly, ANME-1 may be involved in methanogenesis in the strata by first obtaining energy for cell growth and reproduction through AOM to increase its cellular abundance and then occupying a favorable ecological niche with limited resources when sulfate has run out, and the hydrogen concentration has increased. This may have led to a higher relative abundance of ANME-1-THS in methanogenic-dominated terrestrial strata over methanogens (Fig. S7a and b). The inhibition of methanogenesis by salinity was reported to coincide with a reduction in the size of the methanogen population [83]. The present study found that in coastal strata with high salinity levels, the abundance of methanogens was 21.62% lower than in the terrestrial strata (Fig. 3), but the total methane production rate was only 12.05% lower (Fig. 1b), suggesting that potential methanogens in non-Euryarchaeotal lineages may also play a role in methanogenesis. A previous study found a decrease in *mcr*A gene abundance in high-salinity environments [44], consistent with our results (Fig. 4). Since the functional genes for hydrogenotrophic methanogenesis

Fig. 5. Predicted metabolic pathways of different MAGs. **a**, Predicted methanogenesis in the terrestrial Methanofastidiosales MAG. **b**, Predicted AOM in the terrestrial ANME-1-THS MAG. **c**, Predicted metabolic pathway in the terrestrial JS1 MAG. **d**, Predicted AOM in the coastal Methanosarcinales HR1 (ANME-2a/b) MAG. **e**, Predicted AOM in the coastal ANME-1-THS MAG. **f**, Predicted metabolic pathway in the coastal JS1 MAG. The grey color and red font indicate the absence of the enzyme, while black dashed arrow lines indicate the absence of the reaction. A complete list of genes that encode enzymes in the figures can be found in Supporting Information II.

and AOM are the same, it was difficult to determine the methanogenic and AOM activity level based on the abundance of functional genes alone. However, by combining with the results that salinity was significantly and positively correlated with the rate of AOM and the abundance of *mtr*, *mer*, and *mtd* genes (Fig. 1f and Table S4), we hypothesize that salinity increased AOM activity and promoted methane consumption by regulating the abundance of genes involved in AOM.

4.3. Effect of salinity on microbial interactions

Topological characteristics of the stratigraphic archaeal co-occurrence networks indicated that the complexity of the coastal strata network was lower than that of the terrestrial strata (Fig. S5c–e). This is probably because the coastal strata were in an environment of higher salinity stress, where microbial connections tend to be simplified and interactions weaker [84]. In response to salinity stress, the size of the coastal archaeal community co-occurrence network decreased, but modularity increased (Fig. S5c and f). This suggested that archaea may be more sensitive to available resources under such stress and thus adopt an ecological niche differentiation strategy to survive [85]. Based on metabolic pathway analyses, we identified interspecific electron transfer between Atribacteria and methanogens as a potential key biological factor driving stratigraphic CH_4 emissions. Atribacteria JS1 can carry out primary fermentation of carbohydrates or secondary fermentation of organic acids and was often found as the dominant bacterial group in deep sediments with high organic matter content and active methanogenesis [86,87]. As reported, JS1 was abundant in marine sediments, and its proportion of abundance in the bacterial community tended to increase with increasing ocean depth [88–90], demonstrating that JS1 was adapted to higher salinity environments. This was also in accordance with the present study, where the relative abundance of JS1 was greater in coastal strata than in terrestrial strata (Fig. S7d).

Unlike the methylotrophic Methanofastidiosales found in mangrove sediments [91], the Methanofastidiosales identified in this study may produce methane via hydrogenotrophic methanogenesis, with their relative abundance in the terrestrial strata being 90 times greater than in the coastal strata (Fig. S7a). During the anaerobic degradation of organic matter, Methanofastidiosales uses H_2 produced by the fermentation of JS1 to keep the partial pressure of hydrogen low [92]. This, in turn, would allow for the effective and complete degradation of organic matter to H_2 and CO_2 in the presence of JS1. In this way, their interactions would advance methanogenesis in the terrestrial strata. Potential methanogens found in coastal strata were biased towards methylotrophic methanogenesis (Fig. S6d and f), consistent with the reported predominance of the methylotrophic pathway in coastal sediments [93]. Similar to studies in Antarctic Ross Sea sediments, JS1 had the potential to form a syntrophic association with stratigraphic hydrogenotrophic methanogens via acetate oxidation [89]. In the presence of pyruvate formate lyase, acetyl-CoA is produced by the degradation of acetate-formed pyruvate with formate. Pyruvate was aminated to serine, which was further broken down to glycine. Glycine was then cleaved and combined with the tetrahydrofolate (THF) pathway to produce formate. Part of this formate is broken down to CO_2 and H_2 by formate dehydrogenase H (FdhH) and membrane-bound hydrogenase (Mbh). CO_2 and H_2 were then passed on to hydrogenotrophic methanogens for methanogenesis. In addition to Methanofastidiosales, JS1 may also interact with other potential methanogens, such as Nitrososphaeria, and Lokiarchaeia, as reported in previous studies [89,94].

5. Conclusion

This research, grounded in an analysis of methane activity, microbial communities engaged in methane metabolism, and functional genetic elements, advances the hypothesis that the terrestrial shallow gas strata acted as a methane source, while coastal shallow gas strata functioned as a methane sink. In addition, salinity was a key abiotic factor affecting the rate of methane emissions from the strata, alongside the potential importance of interspecific electron transfer between Atribacteria and methanogens as a potential key biotic factor driving methane emissions. This research contributes valuable data for the assessment of global methane emissions and offers theoretical insights that can guide future endeavors related to the exploitation of stratigraphic shallow gas.

CRediT authorship contribution statement

Ying Qu: Conceptualization, Methodology, Visualization, Writing - Original Draft. **Yuxiang Zhao:** Writing - Review & Editing. **Xiangwu Yao:** Methodology, Investigation. **Jiaqi Wang:** Methodology. **Zishu Liu:** Investigation. **Hong Yi:** Resources. **Ping Zheng:** Conceptualization. **Lizhong Wang:** Resources. **Baolan Hu:** Conceptualization, Writing - Review & Editing, Supervision, Funding Acquisition.

Declaration of competing interest

The authors declare that they have no known competing financial interests or personal relationships that could have appeared to influence the work reported in this paper.

Acknowledgments

This work was supported by the Key R&D Program of Zhejiang (No. 2022C03010).

Appendix A. Supplementary data

Supplementary data to this article can be found online at https://doi.org/10.1016/j.ese.2023.100334.

References

[1] J.F. Dean, J.J. Middelburg, T. Rockmann, R. Aerts, L.G. Blauw, M. Egger, M. Jetten, A. de Jong, O.H. Meisel, O. Rasigraf, C.P. Slomp, M.H, In'T. Zandt, A.J. Dolman, Methane Feedbacks to the global climate system in a warmer World, Rev. Geophys. 56 (2018) 207–250, https://doi.org/10.1002/2017RG000559.

[2] IPCC, in: V. Masson-Delmotte, P. Zhai, A. Pirani, S.L. Connors, C. Péan, S. Berger, N. Caud, Y. Chen, L. Goldfarb, M.I. Gomis, M. Huang, K. Leitzell, E. Lonnoy, J.B.R. Matthews, T.K. Maycock, T. Waterfield, O. Yelekçi, R. Yu, B. Zhou (Eds.), Climate Change 2021: the Physical Science Basis. Contribution of Working Group I to the Sixth Assessment Report of the Intergovernmental Panel on Climate Change, Cambridge University Press, Cambridge, United Kingdom and New York, NY, USA, 2021, https://doi.org/10.1017/9781009157896. In press.

[3] X. Lan, K.W. Thoning, and E.J. Dlugokencky. Trends in globally-averaged CH_4, N_2O, and SF_6 determined from NOAA Global Monitoring Laboratory measurements. Version 2023-03, https://doi.org/10.15138/P8XG-AA102023.

[4] X. Lan, S. Basu, S. Schwietzke, L.M.P. Bruhwiler, E.J. Dlugokencky, S.E. Michel, O.A. Sherwood, P.P. Tans, K. Thoning, G. Etiope, Q. Zhuang, L. Liu, Y. Oh, J.B. Miller, G. Pétron, B.H. Vaughn, M. Crippa, Improved Constraints on global methane emissions and sinks using δ^{13}C-CH_4, Global Biogeochem. Cycles 35 (2021), https://doi.org/10.1029/2021GB007000 e2021G-e7000G.

[5] A.G. Judd, M. Hovland, L.I. Dimitrov, S. García Gil, V. Jukes, The geological methane budget at Continental Margins and its influence on climate change, Geofluids 2 (2002) 109–126, https://doi.org/10.1046/j.1468-8123.2002.00027.x.

[6] L. Vielstädte, J. Karstens, M. Haeckel, M. Schmidt, P. Linke, S. Reimann,

V. Liebetrau, D.F. McGinnis, K. Wallmann, Quantification of methane emissions at abandoned gas wells in the Central North Sea, Mar. Petrol. Geol. 68 (2015) 848–860, https://doi.org/10.1016/j.marpetgeo.2015.07.030.
[7] J. Xing, V. Spiess, Shallow gas transport and reservoirs in the vicinity of deeply rooted mud volcanoes in the central Black Sea, Mar. Geol. 369 (2015) 67–78, https://doi.org/10.1016/j.margeo.2015.08.005.
[8] Y. Xu, H. Wu, J.S. Shen, N. Zhang, Risk and impacts on the environment of free-phase biogas in quaternary deposits along the Coastal Region of Shanghai, Ocean Eng. 137 (2017) 129–137, https://doi.org/10.1016/j.oceaneng.2017.03.051.
[9] S. Das, D. Ganguly, S. Chakraborty, A. Mukherjee, T. Kumar De, Methane flux dynamics in relation to methanogenic and methanotrophic populations in the soil of Indian Sundarban mangroves, Mar. Ecol. 39 (2018) e12493, https://doi.org/10.1111/maec.12493.
[10] B. Zhu, C. Karwautz, S. Andrei, A. Klingl, J. Pernthaler, T. Lueders, A novel Methylomirabilota methanotroph potentially couples methane oxidation to iodate reduction, mLife 1 (2022) 323–328, https://doi.org/10.1002/mlf2.12033.
[11] K. Knittel, A. Boetius, Anaerobic oxidation of methane: Progress with an Unknown process, Annu. Rev. Microbiol. 63 (2009) 311–334, https://doi.org/10.1146/annurev.micro.61.080706.093130.
[12] P.N. Evans, J.A. Boyd, A.O. Leu, B.J. Woodcroft, D.H. Parks, P. Hugenholtz, G.W. Tyson, An evolving view of methane metabolism in the Archaea, Nat. Rev. Microbiol. 17 (2019) 219–232, https://doi.org/10.1038/s41579-018-0136-7.
[13] D. Mayumi, H. Mochimaru, H. Tamaki, K. Yamamoto, H. Yoshioka, Y. Suzuki, Y. Kamagata, S. Sakata, Methane production from coal by a single methanogen, Science 354 (2016) 222–225, https://doi.org/10.1126/science.aaf8821.
[14] Z. Lyu, N. Shao, T. Akinyemi, W.B. Whitman Methanogenesis, Curr. Biol. 28 (2018) R727–R732, https://doi.org/10.1016/j.cub.2018.05.021.
[15] Z. Zhou, C. Zhang, P. Liu, L. Fu, R. Laso-Pérez, L. Yang, L. Bai, J. Li, M. Yang, J. Lin, W. Wang, G. Wegener, M. Li, L. Cheng, Non-syntrophic methanogenic hydrocarbon degradation by an archaeal species, Nature 601 (2022) 257–262, https://doi.org/10.1038/s41586-021-04235-2.
[16] K.F. Ettwig, B. Zhu, D. Speth, J.T. Keltjens, M.S.M. Jetten, B. Kartal, Archaea catalyze iron-dependent anaerobic oxidation of methane, Proc. Natl. Acad. Sci. USA 113 (2016) 12792–12796, https://doi.org/10.1073/pnas.1609534113.
[17] P.H.A. Timmers, C.U. Welte, J.J. Koehorst, C.M. Plugge, M.S.M. Jetten, A.J.M. Stams, M.W. Friedrich, Reverse Methanogenesis and Respiration in Methanotrophic Archaea, Archaea, 2017 1654237, https://doi.org/10.1155/2017/1654237, 2017.
[18] L. Shi, T. Guo, P. Lv, Z. Niu, Y. Zhou, X. Tang, P. Zheng, L. Zhu, Y. Zhu, A. Kappler, H. Zhao, Coupled anaerobic methane oxidation and reductive arsenic mobilization in wetland soils, Nat. Geosci. 13 (2020) 799–805, https://doi.org/10.1038/s41561-020-00659-z.
[19] E.I. Valenzuela, K.A. Avendaño, N. Balagurusamy, S. Arriaga, C. Nieto-Delgado, F. Thalasso, F.J. Cervantes, Electron shuttling mediated by humic substances fuels anaerobic methane oxidation and carbon burial in wetland sediments, Sci. Total Environ. 650 (2019) 2674–2684, https://doi.org/10.1016/j.scitotenv.2018.09.388.
[20] G. Ren, A. Ma, Y. Zhang, Y. Deng, G. Zheng, X. Zhuang, G. Zhuang, D. Fortin, Electron acceptors for anaerobic oxidation of methane drive microbial community structure and diversity in mud volcanoes, Environ. Microbiol. 20 (2018) 2370–2385, https://doi.org/10.1111/1462-2920.14128.
[21] A. Schnakenberg, D.A. Aromokeye, A. Kulkarni, L. Maier, L.C. Wunder, T. Richter-Heitmann, T. Pape, P.P. Ristova, S.I. Bühring, I. Dohrmann, G. Bohrmann, S. Kasten, M.W. Friedrich, Electron acceptor availability shapes anaerobically methane oxidizing archaea (ANME) communities in south Georgia sediments, Front. Microbiol. 12 (2021), https://doi.org/10.3389/fmicb.2021.617280.
[22] I. Vanwonterghem, P.N. Evans, D.H. Parks, P.D. Jensen, B.J. Woodcroft, P. Hugenholtz, G.W. Tyson, Methylotrophic methanogenesis discovered in the archaeal phylum *Verstraetearchaeota*, Nat Microbiol 1 (2016) 16170, https://doi.org/10.1038/nmicrobiol.2016.170.
[23] Z. Hua, Y. Wang, P.N. Evans, Y. Qu, K.M. Goh, Y. Rao, Y. Qi, Y. Li, M. Huang, J. Jiao, Y. Chen, Y. Mao, W. Shu, W. Hozzein, B.P. Hedlund, G.W. Tyson, T. Zhang, W. Li, Insights into the ecological roles and evolution of methyl-coenzyme M reductase-containing hot spring Archaea, Nat. Commun. 10 (2019) 4574, https://doi.org/10.1038/s41467-019-12574-y.
[24] M. Cai, Y. Liu, X. Yin, Z. Zhou, M.W. Friedrich, T. Richter-Heitmann, R. Nimzyk, A. Kulkarni, X. Wang, W. Li, J. Pan, Y. Yang, J. Gu, M. Li, Diverse Asgard archaea including the novel phylum *Gerdarchaeota* participate in organic matter degradation, Sci. China Life Sci. 63 (2020) 886–897, https://doi.org/10.1007/s11427-020-1679-1.
[25] L.J. McKay, M. Dlakić, M.W. Fields, T.O. Delmont, A.M. Eren, Z.J. Jay, K.B. Klingelsmith, D.B. Rusch, W.P. Inskeep, Co-occurring genomic capacity for anaerobic methane and dissimilatory sulfur metabolisms discovered in the *Korarchaeota*, Nat Microbiol 4 (2019) 614–622, https://doi.org/10.1038/s41564-019-0362-4.
[26] Y. Wang, G. Wegener, J. Hou, F. Wang, X. Xiao, Expanding anaerobic alkane metabolism in the domain of Archaea, Nat Microbiol 4 (2019) 595–602, https://doi.org/10.1038/s41564-019-0364-2.
[27] J.C. Stegen, X. Lin, A.E. Konopka, J.K. Fredrickson, Stochastic and deterministic assembly processes in subsurface microbial communities, ISME J. 6 (2012) 1653–1664, https://doi.org/10.1038/ismej.2012.22.
[28] J. Zhou, D. Ning, Stochastic community assembly: does it matter in microbial ecology? Microbiol. Mol. Biol. Rev. 81 (2017) e2–e17, https://doi.org/10.1128/MMBR.00002-17.
[29] G. Bell, Neutral macroecology, Science 293 (2001) 2413–2418, https://doi.org/10.1126/science.293.5539.2413.
[30] Y. Deng, Y.H. Jiang, Y.F. Yang, Z.L. He, F. Luo, J.Z. Zhou, Molecular ecological network analyses, BMC Bioinf. 13 (2012), https://doi.org/10.1186/1471-2105-13-113.
[31] Y. Zhao, J. Cai, P. Zhang, W. Qin, Y. Lou, Z. Liu, B. Hu, Core fungal species strengthen microbial cooperation in a food-waste composting process, Environ Sci Ecotech 12 (2022) 100190, https://doi.org/10.1016/j.ese.2022.100190.
[32] X. Yang, L. Zhang, Y. Chen, Q. He, T. Liu, G. Zhang, L. Yuan, H. Peng, H. Wang, F. Ju, Micro(nano)plastic size and concentration co-differentiate nitrogen transformation, microbiota dynamics, and assembly patterns in constructed wetlands, Water Res. 220 (2022) 118636, https://doi.org/10.1016/j.watres.2022.118636.
[33] D. Li, H.W. Ni, S. Jiao, Y.H. Lu, J.Z. Zhou, B. Sun, Y.T. Liang, Coexistence patterns of soil methanogens are closely tied to methane generation and community assembly in rice paddies, Microbiome 9 (2021), https://doi.org/10.1186/s40168-020-00978-8.
[34] Z. Liang, A. Abdillah, W. Fang, R. Qiu, B. Mai, Z. He, P. Juneau, M.P. Gomes, C.R. Priadi, S. Wang, Unique microbiome in organic matter–polluted urban rivers, Global Change Biol. 29 (2023) 391–403, https://doi.org/10.1111/gcb.16472.
[35] L.C. Fan, D. Schneider, M.A. Dippold, A. Poehlein, W.C. Wu, H. Gui, T.D. Ge, J.S. Wu, V. Thiel, Y. Kuzyakov, M. Dorodnikov, Active metabolic pathways of anaerobic methane oxidation in paddy soils, Soil Biol. Biochem. 156 (2021), https://doi.org/10.1016/j.soilbio.2021.108215.
[36] L. Fonseca De Souza, D.O. Alvarez, L.A. Domeignoz-Horta, F.V. Gomes, C. de Souza Almeida, L.F. Merloti, L.W. Mendes, F.D. Andreote, B.J.M. Bohannan, J.L. Mazza Rodrigues, K. Nüsslein, S.M. Tsai, Maintaining grass coverage increases methane uptake in Amazonian pastures, with a reduction of methanogenic archaea in the rhizosphere, Sci. Total Environ. 838 (2022) 156225, https://doi.org/10.1016/j.scitotenv.2022.156225.
[37] H. Cui, X. Su, S. Wei, Y. Zhu, Z. Lu, Y. Wang, Y. Li, H. Liu, S. Zhang, S. Pang, Comparative analyses of methanogenic and methanotrophic communities between two different water regimes in Controlled wetlands on the qinghai-Tibetan plateau, China, Curr. Microbiol. 75 (2018) 484–491, https://doi.org/10.1007/s00284-017-1407-7.
[38] M. Hu, H. Ren, P. Ren, J. Li, B.J. Wilson, C. Tong, Response of gaseous carbon emissions to low-level salinity increase in tidal marsh ecosystem of the Min River estuary, southeastern China, J. Environ. Sci. 52 (2017) 210–222, https://doi.org/10.1016/j.jes.2016.05.009.
[39] H.J. Poffenbarger, B.A. Needelman, J.P. Megonigal, Salinity influence on methane emissions from tidal marshes, Wetlands 31 (2011) 831–842, https://doi.org/10.1007/s13157-011-0197-0.
[40] C. Vizza, W.E. West, S.E. Jones, J.A. Hart, G.A. Lamberti, Regulators of coastal wetland methane production and responses to simulated global change, Biogeosciences 14 (2017) 431–446, https://doi.org/10.5194/bg-14-431-2017.
[41] G. van Dijk, L.P.M. Lamers, R. Loeb, P. Westendorp, R. Kuiperij, H.H. van Kleef, M. Klinge, A.J.P. Smolders, Salinization lowers nutrient availability in formerly brackish freshwater wetlands; unexpected results from a long-term field experiment, Biogeochemistry 143 (2019) 67–83, https://doi.org/10.1007/s10533-019-00549-6.
[42] G.O. Holm, B.C. Perez, D.E. McWhorter, K.W. Krauss, D.J. Johnson, R.C. Raynie, C.J. Killebrew, Ecosystem level methane fluxes from tidal freshwater and brackish marshes of the Mississippi river delta: implications for coastal wetland carbon Projects, Wetlands 36 (2016) 401–413, https://doi.org/10.1007/s13157-016-0746-7.
[43] D.J. Van Horn, J.G. Okie, H.N. Buelow, M.N. Gooseff, J.E. Barrett, C.D. Takacs-Vesbach, Soil microbial responses to increased moisture and organic resources along a salinity gradient in a polar desert, Appl. Environ. Microbiol. 80 (2014) 3034–3043, https://doi.org/10.1128/AEM.03414-13.
[44] S.Z. Chen, P. Wang, H.D. Liu, W. Xie, X.S. Wan, S.J. Kao, T.J. Phelps, C.L. Zhang, Population dynamics of methanogens and methanotrophs along the salinity gradient in Pearl River Estuary: implications for methane metabolism, Appl. Microbiol. Biotechnol. 104 (2020) 1331–1346, https://doi.org/10.1007/s00253-019-10221-6.
[45] C. Dang, E.M. Morrissey, S.C. Neubauer, R.B. Franklin, Novel microbial community composition and carbon biogeochemistry emerge over time following saltwater intrusion in wetlands, Global Change Biol. 25 (2019) 549–561, https://doi.org/10.1111/gcb.14486.
[46] X. Li, D. Gao, L. Hou, M. Liu, Salinity stress changed the biogeochemical controls on CH_4 and N_2O emissions of estuarine and intertidal sediments, Sci. Total Environ. 652 (2019) 593–601, https://doi.org/10.1016/j.scitotenv.2018.10.294.
[47] J. Chen, L. Liu, Z. Wu, S. Tang, R. Liu, X. Zhang, S. Zhang, Shallow acoustic stratigraphy of the late quaternary in the Zhoushan islands of Hangzhou Bay, Marine Geology Letters 37 (2021) 49–57, https://doi.org/10.16028/j.1009-2722.2021.190.
[48] M. Zhou, Z. Liu, B. Zhang, J. Yang, B. Hu, Interaction between arsenic metabolism genes and arsenic leads to a lose-lose situation, Environ. Pollut. 312 (2022) 119971, https://doi.org/10.1016/j.envpol.2022.119971.
[49] T. Xing, P. Liu, M. Ji, Y. Deng, K. Liu, W. Wang, Y. Liu, Sink or source: alternative roles of glacier Foreland meadow soils in methane emission is regulated by

glacier melting on the Tibetan plateau, Front. Microbiol. 13 (2022), https://doi.org/10.3389/fmicb.2022.862242.
[50] A. Hassani, A. Azapagic, N. Shokri, Global predictions of primary soil salinization under changing climate in the 21st century, Nat. Commun. 12 (2021) 6663, https://doi.org/10.1038/s41467-021-26907-3.
[51] K.M. Meyer, A.M. Hopple, A.M. Klein, A.H. Morris, S.D. Bridgham, B. Bohannan, Community structure - ecosystem function relationships in the Congo Basin methane cycle depend on the physiological scale of function, Mol. Ecol. 29 (2020) 1806–1819, https://doi.org/10.1111/mec.15442.
[52] Z. Hu, L. Yang, J. Han, Z. Liu, Y. Zhao, Y. Jin, Y. Sheng, L. Zhu, B. Hu, Human viruses lurking in the environment activated by excessive use of COVID-19 prevention supplies, Environ. Int. 163 (2022) 107192, https://doi.org/10.1016/j.envint.2022.107192.
[53] Y. Cai, Y. Zheng, P.L.E. Bodelier, R. Conrad, Z. Jia, Conventional methanotrophs are responsible for atmospheric methane oxidation in paddy soils, Nat. Commun. 7 (2016) 11728, https://doi.org/10.1038/ncomms11728.
[54] J. Wang, C. Cai, Y. Li, M. Hua, J. Wang, H. Yang, P. Zheng, B. Hu, Denitrifying anaerobic methane oxidation: a previously overlooked methane sink in intertidal zone, Environ. Sci. Technol. 53 (2019) 203–212, https://doi.org/10.1021/acs.est.8b05742.
[55] B.J. Callahan, P.J. McMurdie, M.J. Rosen, A.W. Han, A.J.A. Johnson, S.P. Holmes, DADA2: high-resolution sample inference from Illumina amplicon data, Nat. Methods 13 (2016) 581–583, https://doi.org/10.1038/nmeth.3869.
[56] A. Bolger, M. Lohse, B. Usadel Trimmomatic, A Flexible trimmer for Illumina sequence data, Bioinformatics (2014) 30, https://doi.org/10.1093/bioinformatics/btu170.
[57] D. Li, R. Luo, C. Liu, C. Leung, H. Ting, K. Sadakane, H. Yamashita, T. Lam, MEGAHIT v1.0: a fast and scalable metagenome assembler driven by advanced methodologies and community practices, Methods 102 (2016) 3–11, https://doi.org/10.1016/j.ymeth.2016.02.020.
[58] D.H. Parks, M. Imelfort, C.T. Skennerton, P. Hugenholtz, G.W. Tyson CheckM, Assessing the quality of microbial genomes recovered from isolates, single cells, and metagenomes, Genome Res. 25 (2015) 1043–1055, https://doi.org/10.1101/gr.186072.114.
[59] M. Steinegger, J. Söding, Clustering huge protein sequence sets in linear time, Nat. Commun. 9 (2018) 2542, https://doi.org/10.1038/s41467-018-04964-5.
[60] B. Buchfink, C. Xie, D.H. Huson, Fast and sensitive protein alignment using DIAMOND, Nat. Methods 12 (2015) 59–60, https://doi.org/10.1038/nmeth.3176.
[61] D. Ning, M. Yuan, L. Wu, Y. Zhang, X. Guo, X. Zhou, Y. Yang, A.P. Arkin, M.K. Firestone, J. Zhou, A quantitative framework reveals ecological drivers of grassland microbial community assembly in response to warming, Nat. Commun. 11 (2020) 4717, https://doi.org/10.1038/s41467-020-18560-z.
[62] J. Lai, Y. Zou, J. Zhang, P.R. Peres-Neto, Generalizing hierarchical and variation partitioning in multiple regression and canonical analyses using the rdacca.hp R package, Methods Ecol. Evol. 13 (2022) 782–788, https://doi.org/10.1111/2041-210X.13800.
[63] T. Wen, P. Xie, S. Yang, G. Niu, X. Liu, Z. Ding, C. Xue, Y. Liu, Q. Shen, J. Yuan ggClusterNet, An R package for microbiome network analysis and modularity-based multiple network layouts, iMeta 1 (2022) e32, https://doi.org/10.1002/imt2.32.
[64] Y. Zhao, Q. Weng, B. Hu, Microbial interaction promote the degradation rate of organic matter in thermophilic period, Waste Manage. (Tucson, Ariz.) 144 (2022) 11–18, https://doi.org/10.1016/j.wasman.2022.03.006.
[65] Y. Zhao, Y. Lou, W. Qin, J. Cai, P. Zhang, B. Hu, Interval aeration improves degradation and humification by enhancing microbial interactions in the composting process, Bioresour. Technol. 358 (2022) 127296, https://doi.org/10.1016/j.biortech.2022.127296.
[66] Y. Zhao, J. Wang, Z. Liu, W. Yang, J. Hu, Z. Jia, B. Hu Biofilm, A strategy for the dominance of comammox Nitrospira, J. Clean. Prod. 363 (2022) 132361, https://doi.org/10.1016/j.jclepro.2022.132361.
[67] G. Yang, J. Tian, H. Chen, L. Jiang, W. Zhan, J. Hu, E. Zhu, C. Peng, Q. Zhu, D. Zhu, Y. He, M. Li, F. Dong, Peatland degradation reduces methanogens and methane emissions from surface to deep soils, Ecol. Indicat. 106 (2019) 105488, https://doi.org/10.1016/j.ecolind.2019.105488.
[68] H. Feng, J. Guo, C. Peng, X. Ma, D. Kneeshaw, H. Chen, Q. Liu, M. Liu, C. Hu, W. Wang, Global estimates of forest soil methane flux identify a temperate and tropical forest methane sink, Geoderma 429 (2023) 116239, https://doi.org/10.1016/j.geoderma.2022.116239.
[69] S.R. Padhy, P. Bhattacharyya, S.K. Nayak, P.K. Dash, T. Mohapatra, A unique bacterial and archaeal diversity make mangrove a green production system compared to rice in wetland ecology: a metagenomic approach, Sci. Total Environ. 781 (2021) 146713, https://doi.org/10.1016/j.scitotenv.2021.146713.
[70] J.A. Rosentreter, A.V. Borges, B.R. Deemer, M.A. Holgerson, S. Liu, C. Song, J. Melack, P.A. Raymond, C.M. Duarte, G.H. Allen, D. Olefeldt, B. Poulter, T.I. Battin, B.D. Eyre, Half of global methane emissions come from highly variable aquatic ecosystem sources, Nat. Geosci. 14 (2021) 225–230, https://doi.org/10.1038/s41561-021-00715-2.
[71] P. Yang, K.W. Tang, C. Tong, D. Lai, L.Z. Wu, H. Yang, L.H. Zhang, C. Tang, Y. Hong, G.H. Zhao, Changes in sediment methanogenic archaea community structure and methane production potential following conversion of coastal marsh to aquaculture ponds, Environ. Pollut. 305 (2022), https://doi.org/10.1016/j.envpol.2022.119276.
[72] M.E. Asplund, S. Bonaglia, C. Boström, M. Dahl, D. Deyanova, K. Gagnon, M. Gullström, M. Holmer, M. Björk, Methane emissions from nordic seagrass meadow sediments, Front. Mar. Sci. 8 (2022), https://doi.org/10.3389/fmars.2021.811533.
[73] Y. Yue, Y. Tang, L. Cai, Z. Yang, X. Chen, Y. Ouyang, J. Dai, M. Yang, Co-occurrence relationship and stochastic processes affect sedimentary archaeal and bacterial community assembly in estuarine-coastal margins, Microorganisms 10 (2022) 1339, https://doi.org/10.3390/microorganisms10071339.
[74] K.P. Zhang, Y. Shi, X.Q. Cui, P. Yue, K.H. Li, X.J. Liu, B.M. Tripathi, H.Y. Chu, Salinity is a key determinant for soil microbial communities in a desert ecosystem, mSystems 4 (2019), https://doi.org/10.1128/mSystems.00225-18.
[75] H. Yu, Q. Zhong, Y. Peng, X. Zheng, F. Xiao, B. Wu, X. Yu, Z. Luo, L. Shu, C. Wang, Q. Yan, Z. He, Environmental filtering by pH and salinity jointly drives Prokaryotic community assembly in coastal wetland sediments, Front. Mar. Sci. 8 (2022), https://doi.org/10.3389/fmars.2021.792294.
[76] S. Langenheder, E.S. Lindström, Factors influencing aquatic and terrestrial bacterial community assembly, Env Microbiol Rep 11 (2019) 306–315, https://doi.org/10.1111/1758-2229.12731.
[77] K.M. Rath, J. Rousk, Salt effects on the soil microbial decomposer community and their role in organic carbon cycling: a review, Soil Biol. Biochem. 81 (2015) 108–123, https://doi.org/10.1016/j.soilbio.2014.11.001.
[78] E. Morrissey, J. Gillespie, J. Morina, R. Franklin, Salinity affects microbial activity and soil organic matter content in tidal wetlands, Global Change Biol. 20 (2013), https://doi.org/10.1111/gcb.12431.
[79] E. Magnuson, I. Altshuler, M.Á. Fernández-Martínez, Y. Chen, C. Maggiori, J. Goordial, L.G. Whyte, Active lithoautotrophic and methane-oxidizing microbial community in an anoxic, sub-zero, and hypersaline High Arctic spring, ISME J. 16 (2022) 1798–1808, https://doi.org/10.1038/s41396-022-01233-8.
[80] G. Borrel, P.S. Adam, L.J. McKay, L. Chen, I.N. Sierra-García, C.M.K. Sieber, Q. Letourneur, A. Ghozlane, G.L. Andersen, W. Li, S.J. Hallam, G. Muyzer, V.M. de Oliveira, W.P. Inskeep, J.F. Banfield, S. Gribaldo, Wide diversity of methane and short-chain alkane metabolisms in uncultured archaea, Nat Microbiol 4 (2019) 603–613, https://doi.org/10.1038/s41564-019-0363-3.
[81] T.M. Hoehler, M.J. Alperin, D.B. Albert, C.S. Martens, Thermodynamic control on hydrogen concentrations in anoxic sediments, Geochem. Cosmochim. Acta 62 (1998) 1745–1756, https://doi.org/10.1016/S0016-7037(98)00106-9.
[82] R.T. Kevorkian, S. Callahan, R. Winstead, K.G. Lloyd, ANME-1 archaea may drive methane accumulation and removal in estuarine sediments, Env Microbiol Rep 13 (2021) 185–194, https://doi.org/10.1111/1758-2229.12926.
[83] P. Pattnaik, S.R. Mishra, K. Bharati, S.R. Mohanty, N. Sethunathan, T.K. Adhya, Influence of salinity on methanogenesis and associated microflora in tropical rice soils, Microbiol. Res. 155 (2000) 215–220, https://doi.org/10.1016/S0944-5013(00)80035-X.
[84] C. Li, L. Jin, C. Zhang, S. Li, T. Zhou, Z. Hua, L. Wang, S. Ji, Y. Wang, Y. Gan, J. Liu, Destabilized microbial networks with distinct performances of abundant and rare biospheres in maintaining networks under increasing salinity stress, iMeta (2023) e79, https://doi.org/10.1002/imt2.79.
[85] D.J. Hernandez, A.S. David, E.S. Menges, C.A. Searcy, M.E. Afkhami, Environmental stress destabilizes microbial networks, ISME J. 15 (2021) 1722–1734, https://doi.org/10.1038/s41396-020-00882-x.
[86] M.K. Nobu, J.A. Dodsworth, S.K. Murugapiran, C. Rinke, E.A. Gies, G. Webster, P. Schwientek, P. Kille, R.J. Parkes, H. Sass, B.B. Jørgensen, A.J. Weightman, W. Liu, S.J. Hallam, G. Tsiamis, T. Woyke, B.P. Hedlund, Phylogeny and physiology of candidate phylum '*Atribacteria*' (OP9/JS1) inferred from cultivation-independent genomics, ISME J. 10 (2016) 273–286, https://doi.org/10.1038/ismej.2015.97.
[87] M. Winkel, J. Mitzscherling, P.P. Overduin, F. Horn, M. Winterfeld, R. Rijkers, M.N. Grigoriev, C. Knoblauch, K. Mangelsdorf, D. Wagner, S. Liebner, Anaerobic methanotrophic communities thrive in deep submarine permafrost, Sci Rep-Uk 8 (2018) 1291, https://doi.org/10.1038/s41598-018-19505-9.
[88] S.A. Carr, B.N. Orcutt, K.W. Mandernack, J.R. Spear, Abundant Atribacteria in deep marine sediment from the adelie basin, Antarctica, Front. Microbiol. 6 (2015), https://doi.org/10.3389/fmicb.2015.00872.
[89] Y.M. Lee, K. Hwang, J.I. Lee, M. Kim, C.Y. Hwang, H. Noh, H. Choi, H.K. Lee, J. Chun, S.G. Hong, S.C. Shin, Genomic insight into the predominance of candidate phylum Atribacteria JS1 lineage in marine sediments, Front. Microbiol. 9 (2018), https://doi.org/10.3389/fmicb.2018.02909.
[90] A. Blazejak, A. Schippers, High abundance of JS-1- and Chloroflexi-related Bacteria in deeply buried marine sediments revealed by quantitative, real-time PCR, FEMS Microbiol. Ecol. 72 (2010) 198–207, https://doi.org/10.1111/j.1574-6941.2010.00838.x.
[91] C. Zhang, J. Pan, Y. Liu, C. Duan, M. Li, Genomic and transcriptomic insights into methanogenesis potential of novel methanogens from mangrove sediments, Microbiome 8 (2020) 94, https://doi.org/10.1186/s40168-020-00876-z.
[92] C. Moissl-Eichinger, M. Pausan, J. Taffner, G. Berg, C. Bang, R.A. Schmitz, Archaea are interactive Components of Complex microbiomes, Trends Microbiol. 26 (2018) 70–85, https://doi.org/10.1016/j.tim.2017.07.004.
[93] X. Zhang, C. Zhang, Y. Liu, R. Zhang, M. Li, Non-negligible roles of archaea in coastal carbon biogeochemical cycling, Trends Microbiol. (2022), https://doi.org/10.1016/j.tim.2022.11.008.
[94] Y. Chen, C. Xu, N. Wu, Z. Sun, C. Liu, Y. Zhen, Y. Xin, X. Zhang, W. Geng, H. Cao, B. Zhai, J. Li, S. Qin, Y. Zhou, Diversity of anaerobic methane oxidizers in the Cold seep sediments of the okinawa trough, Front. Microbiol. 13 (2022), https://doi.org/10.3389/fmicb.2022.819187.